Investigation of structural and magnetic properties of Fe-Rh-(Z) (Z = Co, Pt) alloys by first principles method

Oksana Pavlukhina[1,*], *Vladimir* Sokolovskiy[1,2], *Mikhail* Zagrebin[1], *Vasily* Buchelnikov[1]

[1] Chelyabinsk State University, Condensed Matter Physics Department, 454001 Chelyabinsk, Russia
[2] National University of Science and Technology "MIS&S", 119049 Moscow, Russia

Abstract. In this work, we present theoretical investigations of the structural and magnetic properties Fe (Rh, Co) and Fe (Rh, Pt) alloys using the density functional theory. The energy calculations were performed for the 16-atom supercell ($Fe_8Rh_{8-x}Z_x$) with different initial spin configurations. It is shown that a small variation of Pt or Co content leads to change the type of magnetic ordering. It is shown that the ferromagnetic configuration of $Fe_8Rh_{8-x}Co_x$ (x=2, 3) is more energetically favorable as compared with other configurations in austenite. The antiferromagnetic configuration is more energetically favorable for $Fe_8Rh_7Co_1$ alloy. For the $Fe_8Rh_{8-x}Pt_x$ system, the checkerboard-like antiferromagnetic configuration was found to be more energetically favorable. Besides, the addition of Pt into Fe-Rh system slightly changes the optimized lattice parameter and stimulates the martensitic phase transformation.

1 Introduction

Fe-Rh-based alloys showing a metamagnetic phase transition were studied experimentally and theoretically during the last decade [1-7]. This alloys have attracted a lot of attention because of their possible application in magnetic cooling, thermally assisted magnetic recording and spintronic devices [1-3]. Magnetic cooling attracts the attention of scientists around the world. At the present time, a large number of the intermetallic alloys and compounds including Fe-Rh-Z, Mn-Ga-(N, C), La-Ca-Ba-MnO_3 and Ni–Mn–(Ga, In, Sn, Sb) are also promising candidates in magnetic cooling technology [1-9]. The magnetocaloric effect reaches the maximal value at the temperatures of magnetic or magnetostructural phase transitions. Fe-Rh alloys exhibit a metamagnetic phase transition (AFM-FM). The metamagnetic phase transition in Fe-Rh succeeds also the large change in magnetization, which is responsible for a giant magnetocaloric effect (MCE) upon variation of a magnetic field. For $Fe_{49}Rh_{51}$, Nikitin et al. [9] reported for the first time the giant MCE about -13 K at magnetic field change of 2 T using a direct method of measurements. The similar values of MCE for the same composition were successfully repeated in Refs. [4,.5].

It well known, that the magnetic order in FeRh compounds depends strongly on the concentration. Therefore, it is important to study the effect of adding a third element on the magnetic and structural properties of the material. A. Jezierski et. al. [6] study the influence of dopants Co, Pd, Ru and Pl on the magnetic moment and the density of states at the Fermi energy in FeRh alloys. In this article the electronic and magnetic properties of FeRh alloys doped with Co, Pt, Pd Ir and Ru are studied by the TB LMTO-CPA method. The content of the third element in the $FeRh_{1-x}(Z)_x$ alloys was small and amounted to x = 0-0.05. The article says that a significant change of the magnetic moment and the density of states at the Fermi level during the substitution metals.

In this work, we present theoretical investigations of the structural and magnetic properties Fe- Rh-(Z) (Z = Co, Pt) alloys.

2 Computational details

In this work, the structural and magnetic properties of Co- and Pt-doped Fe-Rh alloys are investigated by using the density functional theory calculations as implemented in the Vienna *Ab initio* Simulation (VASP) package [10]. The ab initio calculations have been carried out by using the 16-atom supercell approach with different initial spin configurations. The generalized gradient approximation for the exchange correlation functional in the formulation of Perdew, Burke and Ernzerhof (PBE) was taken into calculations. The performed calculations were semirelativistic and the spin polarization was taken into account for all the cases. In the calculations the automatically generated uniform grid of k-point as in Monkhorst-Pack grids was taken into account. The k-points in the Brillouin zone for self-consistent field cycles were generated with 12^3 meshes for the lattice relaxation calculations and tetragonal distortion.

* Corresponding author: pavluhinaoo@mail.ru

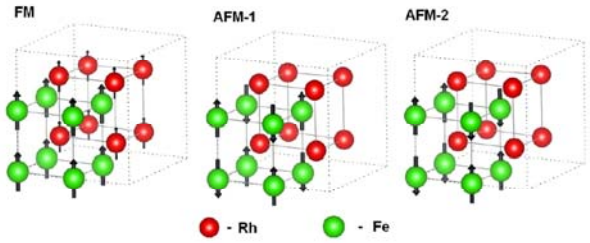

Fig. 1. Spin configurations taken into account in ab initio calculations.

The energy calculations were performed for the $L2_1$ supercell ($Fe_8Rh_{8-x}Z_x$). In detail, original cell has atomic coordinates of (0; 0; 0); (1/2; 0; 0); (1/2; 1/2; 1/2) for Rh atoms and those of (1/4; 1/4; 1/4); (3/4; 3/4; 3/4) for Fe atoms in the supercell. As the result, the supercell contains eight Fe and Rh atoms. Calculations were carried out for ferromagnetic (FM), and two kinds of antiferromagnetic states (AFM-1, AFM-2) with are shown in figures 1. Here, we considered that in the case of FM order the Rh atoms have small magnetic moment (< 1 μB) while it takes zero value for an AFM order.

3 Results of calculations

The variations of the total energy of the 16-atom supercells for $Fe_8Rh_{8-x}Co_x$ (x = 0, 1, 2 and 3) system calculated for different spin configurations as functions of the lattice parameter are presented in figure 2 (a, b, c, d).

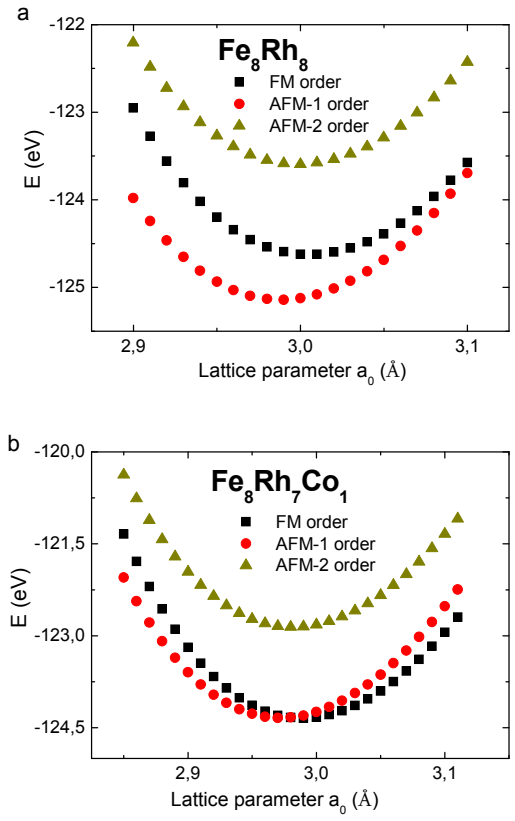

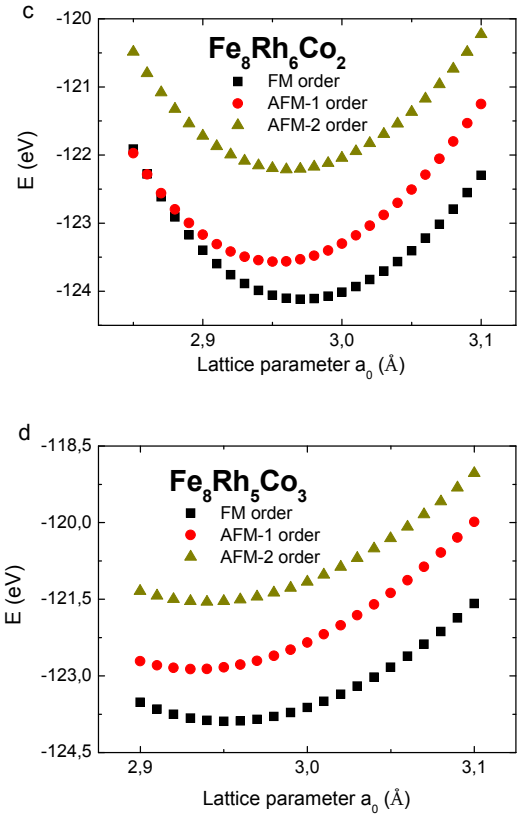

Fig. 2. The total energies of the 16-atom supercells for $Fe_8Rh8\text{-}xCo_x$ system calculated for different spin configurations as functions of the lattice parameter.

We found that the AFM-1 (checkerboard-like) spin configuration in a cubic cell is energetically favorable compared to other AFM and FM configurations from Fe-Rh compound. In this case, a total magnetic moment is found to be of 0 μ_B/f.u. We note that the calculated optimized lattice parameter for Fe-Rh alloy is in a good agreement with experimental and other theoretical values [2, 7]. It is worth noting that for the alloy $Fe_8Rh_7Co_1$ of the energy of the FM and AFM-1 phases are close. However, the antiferromagnetic configuration is more energetically favorable for $Fe_8Rh_7Co_1$ alloy. As can be seen from Figure 2, when cobalt is added, the FM phase becomes energetically favorable. With an increase in the content of cobalt, the FM configuration becomes increasingly more energetically favorable. The total energies of the 16-atom supercells for $Fe_8Rh_{8-x}Pt_x$ system were also calculated for different spin configurations as functions of the lattice parameter. We found that the AFM-1 (checkerboard-like) spin configuration in a cubic cell is energetically favorable compared to other AFM and FM configurations for $Fe_8Rh_{8-x}Pt_x$. In table 1 present the total magnetic moments per formula unit for $Fe_8Rh_{8-x}Pt_x$ (x = 1 – 3) and $Fe_8Rh_{8-x}Co_x$ (x = 1 – 3) at equilibrium lattice parameter for all magnetic configurations. As it can be seen from table 1, the magnetic moments for $Fe_8Rh_{8-x}Pt_x$ (x = 1 – 3) and $Fe_8Rh_{8-x}Co_x$ (x = 1 – 3) are close to 4.0 and 4.2 μ_B/f.u. respectively. Further, we investigated the effect of the addition of the third element on the lattice parameter.

Table 1. The total magnetic moments per formula unit for Fe-Rh-(Z) (Z = Co, Pt) alloys (FM configurations).

x	**Total magnetic moments (μ_B/f. u.) for $Fe_8Rh_{8-x}Co_x$**	**Total magnetic moments (μ_B/f. u.) for $Fe_8Rh_{8-x}Pt_x$**
1	4.251	3.914
2	4.267	4.028
3	4.291	4.128

In Fig. 3 we present the total energy for $Fe_8Rh_{8-x}Co_x$ (x = 1 – 3) system with more energetically favorable spin configuration (AFM-1 for $Fe_8Rh_7Co_1$ and FM for $Fe_8Rh_{8-x}Co_x$ (x = 2 – 3)) and $Fe_8Rh_{8-x}Pt_x$ (x = 1 – 3) system with AFM-1 spin configuration calculated as a function of lattice parameter.'

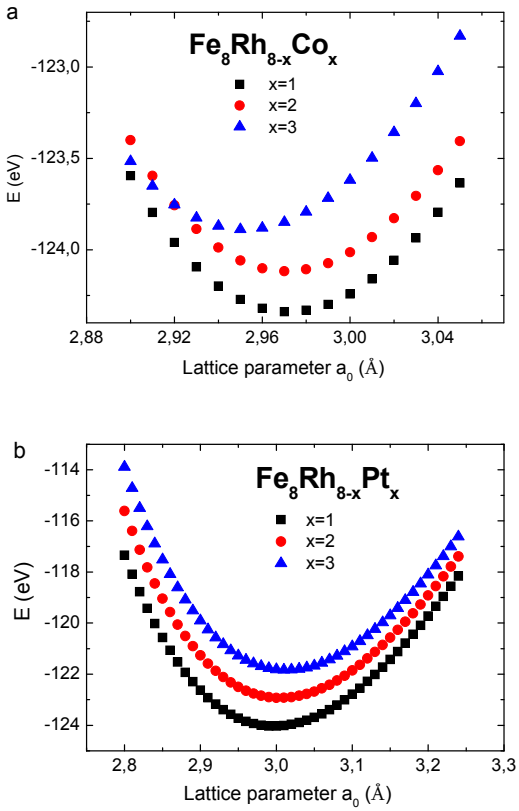

Fig. 3. The total energy curves of the 16-atom supercells in dependence on the lattice parameter for (a) $Fe_8Rh_{8-x}Co_x$ (x = 1 – 3) compositions and (b) for $Fe_8Rh_{8-x}Pt_x$ (x = 1 – 3) system with AFM-1 spin configuration.

Table 2 shows the equilibrium lattice parameters for $Fe_8Rh_{8-x}Pt_x$ (x = 1 – 3) and $Fe_8Rh_{8-x}Co_x$ (x = 1 – 3). Let us consider in more detail the influence of the third element. From the data presented in the table 2, it can be concluded that the addition of Pt atoms leads to an increase in the lattice equilibrium parameter due to the larger atomic radius of Pt compared to the lower Rh value. For cobalt, the reverse is observed. With increasing cobalt content, the equilibrium lattice parameter decreases. This can be explained by the fact that the atomic radius of cobalt is smaller in comparison with rhodium.

Table 2. The lattice parameters depending on the Pt and Co concentration.

x	**Lattice parameter (in Å) for $Fe_8Rh_{8-x}Co_x$**	**Lattice parameter (in Å) for $Fe_8Rh_{8-x}Pt_x$**
1	2.971	2.999
2	2.970	3.00
3	2.951	3.011

Further, the possibility of martensitic transformation in these alloys depending on the third element will be discussed.

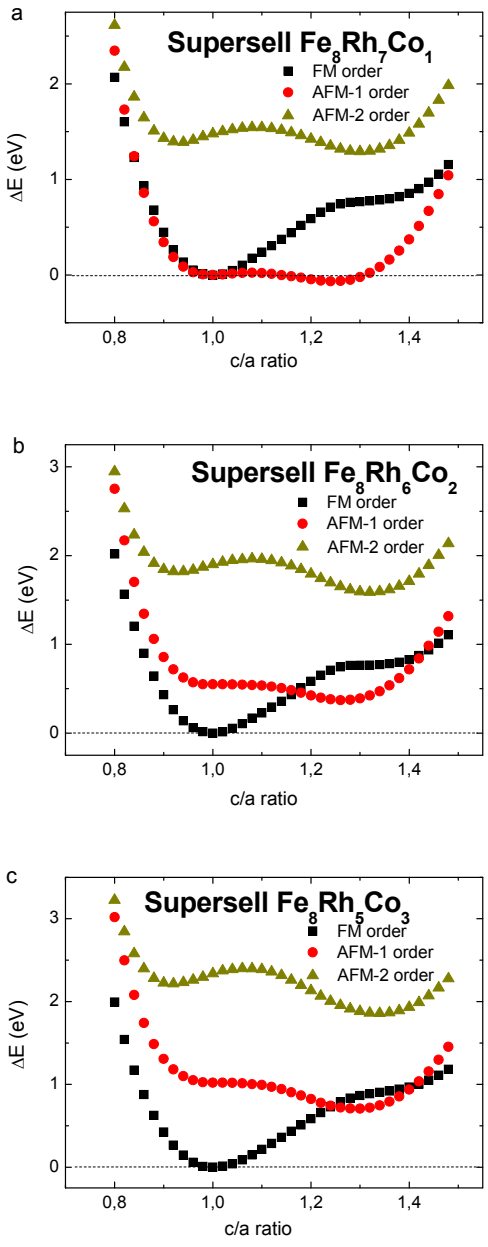

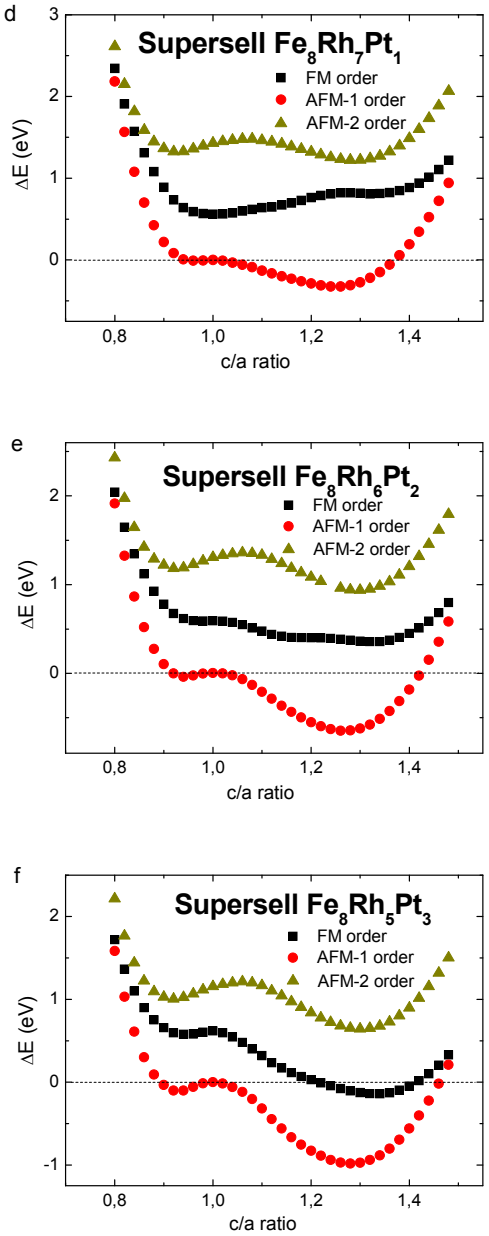

Fig. 4. The variation of the total energy as a function of tetragonal distortion c/a for (a, b, c) $Fe_8Rh_{8-x}Co_x$ (x = 1 – 3) system with FM spin configuration and (d, e, f) $Fe_8Rh_{8-x}Pt_x$ (x = 1 – 3) system with AFM-1 spin configuration.

The calculation of the total energy for the tetragonal distortion of the cubic structure along the *z* axis is performed in this paper. To accomplish this, we fixed the volume of a supercell as $V_0 = a_0^3 \approx a^2c$. The variation of the total energy as a function of tetragonal distortion *c*/*a* for $Fe_8Rh_{8-x}Co_x$ (x = 1 – 3) system and $Fe_8Rh_{8-x}Pt_x$ (x = 1 – 3) one with different spin configuration are shown in Fig. 4 (a-f). In this case, the zero value of ΔE corresponds to the austenitic phase for each compound. Let's consider more in detail the variation of the total energy as a function of tetragonal distortion c/a for $Fe_8Rh_{8-x}Pt_x$ (x = 1 – 3) system with FM, AFM-1 and AFM-2 spin configuration. In the case of $Fe_8Rh_{8-x}Pt_x$, the checkerboard-like antiferromagnetic configuration solution is favorable for martensite states. A tetragonal ratio for martensitic state increases slightly from c/a = 1.26 up to 1.28 with increasing Pt content. Moreover, an increase in Pt content leads to more deeper energy minimum at *c*/*a* ratio. It is important to note that the similar trend was observed experimentally by Yuasa et al. [11]. In the case of $Fe_8Rh_7Co_1$ the checkerboard-like antiferromagnetic configuration solution is favorable for both austenite and martensite states, and the structural transformation occurs without a magnetic phase transition.

4 Conclusion

In summary, the structural and magnetic properties of Co- and Pt-doped Fe-Rh alloys are investigated by using the density functional theory calculations as implemented in the VASP. In a cubic cell the antiferromagnetic configuration is more energetically favorable for $Fe_8Rh_7Co_1$ alloy. It is shown that the ferromagnetic configuration of $Fe_8Rh_{8-x}Co_x$ (x= 2, 3) is more energetically favorable as compared with other configurations in austenite. For the $Fe_8Rh_{8-x}Pt_x$ system, the checkerboard-like antiferromagnetic configuration was found to be more energetically favorable. The addition of Pt into Fe-Rh system slightly changes the optimized lattice parameter and stimulates the martensitic phase transformation with increasing doping concentration Pt due to an appearance of local minima in energy curves.

This work was supported by RSF-Russian Science Foundation No. 17-72-20022\17.

References

1. S. Cumpson, P. Hidding, and R. Coehoorn, IEEE Trans. Magn. **36**, 2271 (2000)
2. J.-U. Thiele, S. Maat, and E. E. Fullerton, Appl. Phys. Lett. **82**, 2859 (2003)
3. A. X. Gray, D.W. Cooke, P. Kruger, Phys. Rev. Lett. **108**, 257208 (2012)
4. M.P. Annaorazov, K.A. Asatryan, G. Myalikgulyev et al. Cryog. **32**, 867 (1992)
5. A. Chirkova, K.P. Skokov, L. Schultz et al. Acta Mater. **106**, 15 (2016)
6. A. Jezierski, G. Borstel. J. Magnet. Magnetic Mater. **140-144**, 81 (2005)
7. O. Pavlukhinaa, V. Sokolovskiy, V. Buchelnikov, Materials Today: Proceedings. **4**. 4642 (2017)
8. O. Pavlukhinaa, V. Sokolovskiy, V. Buchelnikov, Phys. Status Solidi A 213. **2**, 390 (2016)
9. S.A. Nikitin, G. Myalikgulyev, A.M. Tishin, et al., Phys. Lett A. **148**, 363 (1990).
10. G. Kresse and J. Furthmuller, Phys. Rev. B. **54**, 11169 (1996)
11. S. Yuasa, H. Miyajima, Y. Otani, J. Phys. Soc. Jpn. **63**, 3129 (1994)